

Three-Dimensional Numerical Simulation of the Inverse Problem of Thermal Convection

A. T. Ismail-Zadeh^{1,2}, A. I. Korotkii³, B. M. Naimark¹, and I. A. Tsepelev³

¹ *International Institute of Earthquake Prediction Theory and Mathematical Geophysics, Russian Academy of Sciences, Varshavskoe sh. 79 korpus 2, Moscow, 117556 Russia*

² *Geophysikalisches Institut der Universität Karlsruhe, Hertzstrasse 16, D-76187 Karlsruhe, Germany*

³ *Institute of Mathematics and Mechanics, Ural Division, Russian Academy of Sciences, ul. S. Kovalevskoi 16, Yekaterinburg, 620219 Russia*

e-mails: aismail@mitp.ru; korotkii@imm.uran.ru; naimark@mitp.ru; tsepelev@imm.uran.ru

Received June 24, 2002

Abstract—Both forward and inverse (time-reversed) three-dimensional simulations of slow thermoconvective flow are considered for a highly viscous fluid with temperature-dependent density and viscosity. The model is described by the equations of quasi-steady viscous inhomogeneous incompressible flow, advection equations for density and viscosity, and a heat equation. The numerical solution is based on the introduction of a two-component vector velocity potential and on the application of a finite element method with a tricubic-spline basis for computing the potential. The advection equations were solved by the method of characteristics. The heat equation was solved forward in time by a finite-difference method based on a tridiagonal algorithm with the Crank–Nicolson scheme employed in each direction. It was solved backwards in time by a variational method essentially based on a solution of a series of forward problems. The numerical algorithms were designed to be implemented on parallel computers. The principal results of the study are summarized as follows: a numerical method is developed for simultaneous solution of the Stokes flow equation, heat equation, and advection equations for physical parameters of the fluid both forward and backwards in time. Substantial progress in these problems was achieved by using a special representation of the vector velocity potential and choosing a special basis in the finite element method, which resulted in a considerable reduction of numerical complexity. Characteristic examples were computed.

INTRODUCTION

We consider a numerical approach to simulation of three-dimensional forward and inverse problems of thermal convection in an inhomogeneous viscous incompressible fluid. In the forward problem of thermal convection in a continuous medium, a future state of the medium is to be determined from its current state. In mathematical terms, the problem is formulated as follows: find a solution to the system of equations describing the state of the medium (the Stokes flow equation, the continuity equation, advection equations for density and viscosity, and a heat equation) under appropriate boundary and initial conditions by computing forward in time [1–5]. In the inverse problem of thermal convection in a continuous medium, one must recover the history of its motion resulting from the development of disturbances induced by gravity and thermal fields. In other words, the problem is to restore the state of the medium under appropriate boundary and initial conditions by computing backwards in time.

Problems of this kind arise, for example, when the evolution of salt in the crust, mantle convection movement of continents driven by thermoconvective flow in the mantle, or some other geophysical processes are to be modeled. One particular task of interest is the three-dimensional simulation of the incipience, development, and formation of a mantle plume (diapir) caused by internal gravitational instability of an inhomogeneous medium (which can be due to thermally induced expansion of lower layers of the medium or to decrease in density caused by phase transformations). Refinement of methods for processing seismic (or other) probing data makes it possible to study these phenomena in more detail. Simultaneous analysis of these data and results of numerical simulations leads to a better understanding of the nature of the phenomena in question.

Dynamics of inhomogeneous (e.g., salt) structures lies in the focus of studies conducted by geophysicists and geologists, particularly those specializing in deformation of sedimentary rocks, mining engineering, prospecting, and underground construction. The reason is that such formations can promote caving, provide

traps for hydrocarbons, and serve as radioactive waste disposal sites. For example, studies of salt domes are of economic importance. Almost all oil and gas reserves in the Caspian salt basin are associated with salt structure. To understand the history of sediment buildup, erosion, and deformation in sedimentary basins, one must reconstruct the basin's evolution backwards in time. The method of paleoreconstruction, which is frequently employed for these purposes (e.g., see [6]), is a reliable tool for reconstructing the evolution. However, it cannot be applied to restore the history of a salt basin in which salt has deformed the above-lying rock. In [7–9], a numerical approach to a two-dimensional inverse problem of Rayleigh–Taylor instability was presented and the geological and geophysical profiles were numerically reconstructed along the eastern part of the Caspian basin. A numerical approach to the three-dimensional inverse problem of Rayleigh–Taylor instability was presented in [10]. However, the approach to the inverse problem developed in those studies did not take into account any influence of the thermal fields and internal heat sources due to viscous friction. In this paper, we propose a possible approach to the reconstruction problem, based on a three-dimensional computer simulation of the aforementioned inverse problem taking into account thermal effects.

We describe a numerical algorithm designed to solve a class of problems in thermal convection both forward and backwards in time and to reconstruct the evolution of inhomogeneous media, such as salt basins. The analysis is focused on computing the problem backwards in time. In an inhomogeneous structure, small disturbances of layer boundaries or densities lead to its deformation. In the case of inverse density stratification, these disturbances grow into diapiric structures. Mathematically, the problem is stable as computed forward in time: small errors in specifying physical quantities and input data lead to small errors in reconstructing the final state of the medium on a virtually unbounded time interval. In [11, 12], it was proved that the corresponding mathematical problem is well posed in the two-dimensional case. According to [10], a similar assertion is true in the three-dimensional case. However, the corresponding problem is unstable backwards in time: small errors in specifying physical quantities or numerical inaccuracies in computations can lead to large errors in reconstructing the initial state of the medium even over relatively short time intervals. Therefore, it should be solved by invoking methods developed for ill-posed problems.

The equations of motion are approximated numerically by using a finite element method with a tricubic-spline basis. The heat balance equation is approximated by a finite-difference method. The transport equations are solved by the method of characteristics. Some results concerning solution and modeling of forward problems were presented in [13–18]. The solution of the heat equation backwards in time is reduced to the solution of a special variational problem, which is, in turn, reduced to a series of forward problems. These problems are stable with respect to input data perturbations. Under a special choice of numerical approximation, they are stable with respect to computational errors as well. In the present case, the forward heat balance problems were solved by using a tridiagonal algorithm with the second-order accurate Crank–Nicolson scheme employed in each direction [4, 5]. Numerical solution of such problems is a formidable task, because the corresponding discrete approximations have large dimensions. Some progress here was achieved by using special basis elements in the finite element method, a two-component representation of the vector velocity potential, and a special variational method for solving the inverse problem for the heat balance equation. These techniques made it possible to obtain qualitatively and quantitatively adequate results for relatively low-dimensional discrete approximations.

The modeling involved the following basic simplifications: the motion of a viscous inhomogeneous fluid was assumed to be slow, the medium was treated as a Newtonian fluid, and lateral forces (associated with expansion or compression of the medium) were not taken into consideration.

Computations have shown that the proposed methods and algorithms can be applied in numerical implementations of the problems considered here. At the end of the paper, we present the results obtained by solving two model problems.

1. MATHEMATICAL FORMULATION OF SIMULATION PROBLEMS

In the parallelepiped $\Omega = (0, l_1) \times (0, l_2) \times (0, l_3) \subset \mathbb{R}^3$, consider a slow inhomogeneous viscous incompressible flow in the presence of a gravity field. In Cartesian coordinates, the flow obeys the following equations (see [1–3]):

the Stokes flow equation

$$\nabla p = \operatorname{div}(\mu e_{ij}) + \mathbf{F}, \quad (1.1)$$

the incompressibility condition

$$\operatorname{div} \mathbf{u} = \partial u_1 / \partial x_1 + \partial u_2 / \partial x_2 + \partial u_3 / \partial x_3 = 0, \quad (1.2)$$

the heat equation

$$\rho_* c \partial T / \partial t + \rho_* c \langle \mathbf{u}, \nabla T \rangle = \operatorname{div}(k \nabla T) + \mu_* \Phi + \rho Q, \quad (1.3)$$

the equation of state for density

$$\rho(t, x) = \rho_*(t, x) [1 - \alpha(T(t, x) - T_s)], \quad (1.4)$$

the rheological equation for viscosity

$$\mu(t, x) = \mu_*(t, x) \exp\left(\frac{E + \rho_* g x_3 V}{RT} - \frac{E + \rho_s g l_s V}{RT_s}\right), \quad (1.5)$$

and the advection equations for thermally unperturbed density and viscosity

$$\partial \rho_* / \partial t + \langle \nabla \rho_*, \mathbf{u} \rangle = 0, \quad \partial \mu_* / \partial t + \langle \nabla \mu_*, \mathbf{u} \rangle = 0. \quad (1.6)$$

Here, $\mathbf{u} = (u_1, u_2, u_3)$ is the velocity vector; $\mathbf{F} = (0, 0, -g\rho)$ is the external body force per unit volume; g is the gravitational acceleration; p is pressure; ρ is density; μ is viscosity; ρ_* is the thermally unperturbed density; μ_* is the thermally unperturbed viscosity; $e_{ij} = \partial u_i / \partial x_j + \partial u_j / \partial x_i$ is the rate-of-strain tensor; ∇ denotes the gradient operator; div denotes the divergence operator; T is temperature; c is specific heat; k is heat conductivity; Q is the rate of heat production per unit volume due to nonviscous heat sources; E is activation energy; V is activation volume; R is the universal gas constant; α is the coefficient of thermal expansion; ρ_s , l_s , and T_s are the reference density, length, and temperature, respectively; and Φ represents the rate of heat production due to viscous friction:

$$\Phi = 2\left(\frac{\partial u_1}{\partial x_1}\right)^2 + 2\left(\frac{\partial u_2}{\partial x_2}\right)^2 + 2\left(\frac{\partial u_3}{\partial x_3}\right)^2 + \left(\frac{\partial u_2}{\partial x_1} + \frac{\partial u_1}{\partial x_2}\right)^2 + \left(\frac{\partial u_3}{\partial x_1} + \frac{\partial u_1}{\partial x_3}\right)^2 + \left(\frac{\partial u_2}{\partial x_3} + \frac{\partial u_3}{\partial x_2}\right)^2.$$

Equations (1.1)–(1.6) make up a closed set of equations that determine the unknown $u_1, u_2, u_3, T, p, \rho$, and μ as functions of the independent variables t (time) and $x = (x_1, x_2, x_3)$ (Cartesian coordinates of a point in space).

The function u must satisfy prescribed boundary conditions, the function T must satisfy prescribed boundary and initial (or terminal) conditions, and the functions μ_* and ρ_* must satisfy prescribed initial (or terminal) conditions.

On the boundary Γ of the domain Ω , we set the no-slip condition

$$\mathbf{u} = 0, \quad x \in \Gamma \quad (1.7)$$

or the impermeability conditions with perfect slip

$$\langle \mathbf{u}, \mathbf{n} \rangle = 0, \quad \partial \mathbf{u}_\tau / \partial \mathbf{n} = 0, \quad x \in \Gamma, \quad (1.8)$$

where \mathbf{n} is the outward unit normal vector at $x \in \Gamma$ and \mathbf{u}_τ is the projection of the velocity vector onto the tangent plane to Γ at $x \in \Gamma$.

On each face $\Gamma(x_i = 0)$ or $\Gamma(x_i = l_i)$ ($i = 1, 2, 3$) of the parallelepiped Ω , temperature satisfies either a boundary condition of the first kind (Dirichlet condition)

$$T = W_1, \quad (1.9)$$

where W_1 is a prescribed temperature distribution over the boundary segment, or a boundary condition of the second kind (Neumann condition)

$$\partial T / \partial \mathbf{n} = W_2, \quad (1.10)$$

where W_2 is a prescribed heat flux across the boundary segment. In practice, these conditions are frequently combined: temperature is prescribed on some boundary segments; heat flux, on the remaining ones.

To solve the problem forward in time, we set an initial condition for temperature (the initial time is set to zero):

$$T(0, x_1, x_2, x_3) = T_0(x_1, x_2, x_3), \quad x = (x_1, x_2, x_3) \in \Omega, \quad (1.11)$$

where T_0 is a function defined on Ω to specify the temperature distribution over Ω at the initial time.

To solve the problem backwards in time, we prescribe the temperature at the final instant $t = \vartheta$:

$$T(\vartheta, x_1, x_2, x_3) = T_\vartheta(x_1, x_2, x_3), \quad x = (x_1, x_2, x_3) \in \Omega, \quad (1.12)$$

where T_ϑ is a function defined on Ω to specify the temperature distribution over Ω at the final instant.

The initial conditions for the thermally unperturbed density and viscosity have the form

$$\rho_*(0, x) = \rho_0(x), \quad \mu_*(0, x) = \mu_0(x), \quad x \in \Omega, \quad (1.13)$$

where ρ_0 and μ_0 are functions defined on Ω to specify the density and viscosity distributions over Ω at the initial time.

When the problem is to be solved backwards in time, we set terminal conditions for the thermally unperturbed density and viscosity:

$$\rho_*(\vartheta, x) = \rho_\vartheta(x), \quad \mu_*(\vartheta, x) = \mu_\vartheta(x), \quad x \in \Omega, \quad (1.14)$$

where ρ_ϑ and μ_ϑ are functions defined on Ω to specify the density and viscosity distributions over Ω at the final time.

Thus, the forward problem is to compute the functions $\mathbf{u} = \mathbf{u}(t, x)$, $T = T(t, x)$, $\rho = \rho(t, x)$, and $\mu = \mu(t, x)$ that satisfy Eqs. (1.1)–(1.6) in Ω at $t \geq 0$, boundary conditions (1.7)–(1.10), and initial conditions (1.11) and (1.13).

The inverse problem is to compute the functions $\mathbf{u} = \mathbf{u}(t, x)$, $T = T(t, x)$, $\rho = \rho(t, x)$, and $\mu = \mu(t, x)$ that satisfy Eqs. (1.1)–(1.6) in Ω at $t \leq \vartheta$, boundary conditions (1.7)–(1.10), and terminal conditions (1.12) and (1.14).

2. NUMERICAL SCHEME FOR MODEL PROBLEMS

To facilitate computations, Eqs. (1.1)–(1.6) are simplified by introducing a two-component representation of the vector velocity potential,

$$\mathbf{u} = \text{curl}\boldsymbol{\Psi}, \quad \boldsymbol{\Psi} = (\psi_1, \psi_2, 0); \quad (2.1)$$

applying the curl operator to Eq. (1.1); and rewriting Eqs. (1.1)–(1.6) and the quantities contained therein in dimensionless form. These transformations were performed in detail in [14].

Methods for solving forward problems were exposed in [13–18]; methods for solving the Stokes flow equation and the transport equations backwards in time, in [10].

2.1. Variational Method for Solving the Inverse Problem for the Heat Balance Equation

Consider the nonnegative quadratic functional

$$J(\boldsymbol{\varphi}) = \int_{\Omega} |T(\vartheta, x; \boldsymbol{\varphi}) - \chi(x)|^2 dx,$$

where $T(\vartheta, \cdot; \boldsymbol{\varphi})$ is the solution to forward problem (1.3) at the final time ϑ obtained for a (yet unknown) initial temperature distribution $\boldsymbol{\varphi} = \boldsymbol{\varphi}(\cdot)$ and $\chi(\cdot) = T(\vartheta, \cdot; T_0)$ is the known temperature distribution at the final time corresponding to the initial temperature $T_0 = T_0(\cdot)$. We seek the minimum of the functional with respect to the argument $\boldsymbol{\varphi}$. It is clear that the minimal (zero) value of the functional is attained only at the element $\boldsymbol{\varphi} = T_0$ (its uniqueness is due to the uniqueness of the solution to the corresponding boundary value problem for the heat equation):

$$J(T_0) = 0.$$

The minimum can be determined by the gradient method (e.g., see [19]). First, we calculate the gradient of the functional J . We add an increment h to the argument $\boldsymbol{\varphi}$ and define $T(\cdot, \cdot; \boldsymbol{\varphi})$ and $T(\cdot, \cdot; \boldsymbol{\varphi} + h)$ as the solutions to the corresponding forward problems. It is obvious that $z = T(\cdot, \cdot; \boldsymbol{\varphi} + h) - T(\cdot, \cdot; \boldsymbol{\varphi})$ solves the following boundary value problem:

$$\begin{aligned} \rho_* c \partial z / \partial t + \rho_* c \langle \mathbf{u}, \nabla z \rangle &= \text{div}(k \nabla z) - \rho_* \alpha z Q, \quad x \in \Omega, \quad t \in (0, \vartheta), \\ \sigma_1 z + \sigma_2 \partial z / \partial \mathbf{n} &= 0, \quad x \in \Gamma, \quad t \in (0, \vartheta), \\ z(0, x) &= h, \quad x \in \Omega. \end{aligned} \quad (2.2)$$

Here, σ_1 and σ_2 are sufficiently smooth functions or constants such that $\sigma_1^2 + \sigma_2^2 \neq 0$. Adjusting these functions appropriately, one can always satisfy the boundary conditions set in the original formulation of the problem.

The increment of the functional can be represented as

$$\begin{aligned} J(\varphi + h) - J(\varphi) &= \int_{\Omega} |T(\vartheta, x; \varphi + h) - \chi(x)|^2 dx - \int_{\Omega} |T(\vartheta, x; \varphi) - \chi(x)|^2 dx \\ &= 2 \int_{\Omega} [T(\vartheta, x; \varphi) - \chi(x)]z(\vartheta, x) dx + \int_{\Omega} z(\vartheta, x)^2 dx. \end{aligned}$$

Let us show that

$$2 \int_{\Omega} [T(\vartheta, x; \varphi) - \chi(x)]z(\vartheta, x) dx = \int_{\Omega} \Psi(0, x)h(x) dx,$$

where $\Psi = \Psi(\cdot)$ solves the following problem (which is frequently called the conjugate of (2.2) and can be transformed into a forward problem by reversing time):

$$\begin{aligned} \partial\Psi/\partial t + \langle \mathbf{u}, \nabla\Psi \rangle &= -\text{div}[k\nabla(\Psi/\rho_*c)] + \alpha\Psi Q/c, \quad x \in \Omega, \quad t \in (0, \vartheta), \\ \sigma_1(\Psi/\rho_*c) + \sigma_2\partial(\Psi/\rho_*c)/\partial\mathbf{n} &= 0, \quad x \in \Gamma, \quad t \in (0, \vartheta), \\ \Psi(\vartheta, x) &= 2[T(\vartheta, x; \varphi) - \chi(x)], \quad x \in \Omega. \end{aligned} \tag{2.3}$$

Indeed,

$$\int_{\Omega} \Psi(\vartheta, x)z(\vartheta, x) dx = \int_{\Omega} \int_0^{\vartheta} \frac{\partial}{\partial t}(\Psi(t, x)z(t, x)) dx dt + \int_{\Omega} \Psi(0, x)h(x) dx.$$

Since $\Psi = \Psi(\cdot)$ solves problem (2.3) and $z = z(\cdot)$ solves problem (2.2), one can use the boundary conditions in (2.3) and (2.2), the condition $\text{div } \mathbf{u} = 0$, and the boundary conditions for the velocity field to obtain

$$\begin{aligned} \int_{\Omega} \int_0^{\vartheta} \frac{\partial}{\partial t}(\Psi(t, x)z(t, x)) dt dx &= \int_{\Omega} \int_0^{\vartheta} \left\{ \frac{\partial}{\partial t} \Psi(t, x)z(t, x) + \Psi(t, x) \frac{\partial z(t, x)}{\partial t} \right\} dx dt \\ &= \int_{\Omega} \int_0^{\vartheta} z \left[-\langle \mathbf{u}, \nabla\Psi \rangle - \text{div} \left(k\nabla \left(\frac{\Psi}{\rho_*c} \right) \right) + \frac{\alpha}{c} \Psi Q \right] dx dt + \int_{\Omega} \int_0^{\vartheta} \Psi \left[-\langle \mathbf{u}, \nabla z \rangle + \frac{1}{\rho_*c} \text{div}(k\nabla z) + \frac{\alpha}{c} z Q \right] dx dt \\ &= \int_{\Omega} \int_0^{\vartheta} \left\{ k \left(\frac{\Psi}{\rho_*c} \right) \langle \nabla z, \mathbf{n} \rangle - kz \left\langle \nabla \left(\frac{\Psi}{\rho_*c} \right), \mathbf{n} \right\rangle \right\} d\Gamma dt + \int_{\Omega} \int_0^{\vartheta} k \left\{ \left\langle \nabla \left(\frac{\Psi}{\rho_*c} \right), \nabla z \right\rangle - \left\langle \nabla z, \nabla \left(\frac{\Psi}{\rho_*c} \right) \right\rangle \right\} dx dt \\ &\quad + \int_{\Omega} \int_0^{\vartheta} \{ z\Psi \text{div } \mathbf{u} + \Psi \langle \mathbf{u}, \nabla z \rangle - \Psi \langle \mathbf{u}, \nabla z \rangle \} dx dt - \int_{\Omega} \int_0^{\vartheta} z\Psi \langle \mathbf{u}, \mathbf{n} \rangle d\Gamma dt = 0. \end{aligned}$$

Finally, we have

$$J(\varphi + h) - J(\varphi) = \int_{\Omega} \Psi(0, x)h(x) dx + \int_{\Omega} z(\vartheta, x)^2 dx = \langle \Psi(0, \cdot), h \rangle_{L^2(\Omega)} + o(\|h\|_{L^2(\Omega)}).$$

This representation implies that the value of the gradient of J at φ is $\Psi(0, \cdot)$, where Ψ is the solution to boundary value problem (2.3):

$$J'(\varphi) = \Psi(0, \cdot).$$

To minimize the functional J , we invoke the gradient method (see [19])

$$\varphi_{k+1} = \varphi_k - \alpha_k J'(\varphi_k), \quad \varphi_0 = T_s, \quad k = 0, 1, \dots, \tag{2.4}$$

$$\alpha_k = \min\{0.5; J(\varphi_k)/\|J'(\varphi_k)\|_{L^2(\Omega)}\}. \tag{2.5}$$

The numerical scheme for solving the heat equation backwards in time is as follows:

(1) on the time interval $[0, \vartheta]$, find a solution to the forward boundary value problem (1.3), (1.9)–(1.11) supplemented with the initial condition φ_k by using a tridiagonal algorithm with the Crank–Nicolson scheme employed in each direction;

(2) find the gradient $\Psi(0, \cdot)$ of the functional J at the point φ_k by solving problem (2.3) backwards in time with the use of the finite-difference scheme employed in the preceding step;

(3) evaluate the parameter α_k by applying formula (2.5) and use formula (2.4) to update the value of φ_{k+1} (the choice of α_k can be simplified as done in [19]);

(4) if $\|\varphi_k - \varphi_{k+1}\|_{L^2(\Omega)} < \varepsilon$, then terminate the computation and adopt φ_k as an approximation of the unknown initial state of the medium; otherwise, go to step (1) and perform another iteration cycle (in our computations, we used $\varepsilon = 10^{-8}$).

Thus, solution of the inverse heat balance problem is actually reduced to solution of a series of forward problems, which are known to be well posed (see [4, 5]). An analogous method can be applied to solve a similar problem on any time interval.

2.2. Numerical Method for Solving the Stokes Flow Equation

Following the method developed in [14], we represent the vector velocity potential as a linear combination of tricubic basis splines and apply the finite element method to problem (1.1), (1.2), (1.7), (1.8). To simplify analysis, we begin with representing the problem in variational form [14]. To solve the problem numerically, we discretize the domain Ω by introducing the uniform rectangular grid

$$0 = x_i^0 < \dots < x_i^{n_i} = l_i, \quad i = 1, 2, 3,$$

with grid points $\Omega_{ijk} = (x_1^i, x_2^j, x_3^k)$ ($0 \leq i \leq n_1, 0 \leq j \leq n_2, 0 \leq k \leq n_3$). At each grid point Ω_{ijk} , we define a tricubic basis element $\omega_{ijk}^l = \omega_{ijk}^l(x_1, x_2, x_3)$ ($l = 1, 2$) as the tensor product of the corresponding one-dimensional cubic basis elements (see Fig. 1). The construction of bases consisting of tricubic and trilinear elements, ω_{ijk}^l and φ_{ijk}^l , was described in detail in [15, 16].

The vector velocity potential is approximated by the combinations

$$\Psi_l(t, x_1, x_2, x_3) \approx \sum_i \sum_j \sum_k \Psi_{ijk}^l(t) \omega_i^{l1}(x_1) \omega_j^{l2}(x_2) \omega_k^{l3}(x_3), \quad l = 1, 2. \quad (2.6)$$

Density and viscosity are approximated by using trilinear basis elements:

$$\begin{aligned} \rho(t, x_1, x_2, x_3) &\approx \sum_i \sum_j \sum_k \rho_{ijk}(t) \varphi_i^1(x_1) \varphi_j^2(x_2) \varphi_k^3(x_3), \\ \mu(t, x_1, x_2, x_3) &\approx \sum_i \sum_j \sum_k \mu_{ijk}(t) \varphi_i^1(x_1) \varphi_j^2(x_2) \varphi_k^3(x_3). \end{aligned}$$

The coefficients Ψ_{ijk}^l are determined on each time layer by solving a system of linear algebraic equations with a large symmetric positive definite banded matrix. The system is solved iteratively by conjugate gradient methods or by block Gauss–Seidel (over- or underrelaxation) methods. This is done by grouping the grid points Ω_{ijk} into blocks and distributing them among processors so that each processor is associated with at least three grid points in the x_1 direction. When a distributed-memory parallel computer is employed, an important role is played by the distribution of data among processors, which determines the final amount of data handled by each processor and data exchange between processors. To optimize the distribution, the amounts of data handled and stored should be equal for each processor, while the exchange between the processors should be minimized. The partition into blocks shown in Fig. 2 minimizes data exchange between the processors. Detailed analyses of particular implementations of iterative methods for systems of linear algebraic equations having this structure were presented in [13, 14].

2.3. Numerical Method for Solving the Advection Equations

The advection equations have characteristics described by the system of ordinary differential equations

$$dx(t)/dt = \mathbf{u}(t, x(t)).$$

Both density and viscosity retain constant values along the characteristics:

$$\rho_*(t, x(t)) = \rho_0(x(0)), \quad \mu_*(t, x(t)) = \mu_0(x(0)).$$

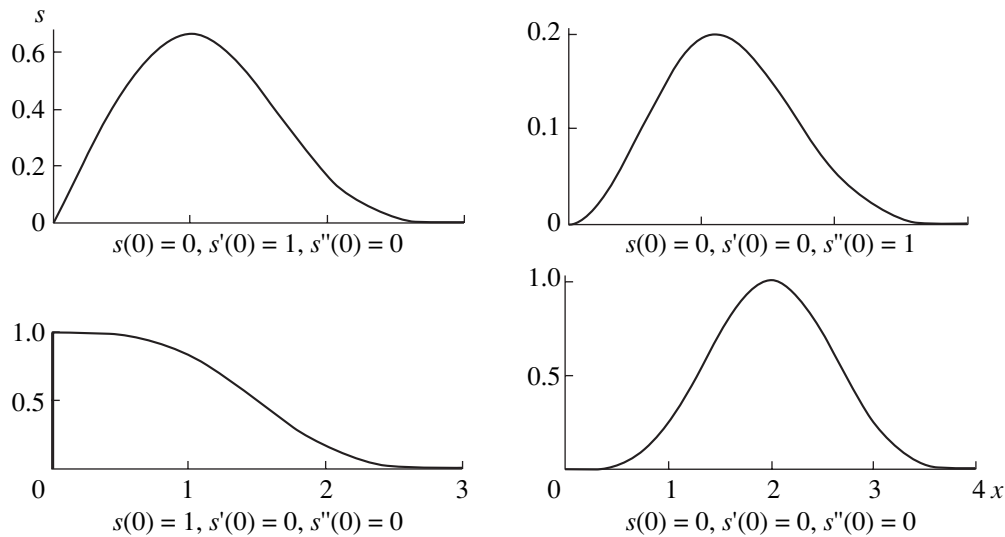


Fig. 1.

These formulas can be used to determine the density and viscosity at a time t for known density and viscosity distributions at the initial time and for known velocity fields prior to t , which must have already been computed. Applying trilinear basis elements to approximate density and viscosity, one can organize a sufficiently large number of independent modules to perform parallel computations of the characteristics of the transport equations. Computations of density and viscosity backwards in time are performed in a similar manner.

2.4. Numerical Method for Solving the Heat Equation

Temperature is approximated by finite-difference methods. To do this, we define a regular grid in Ω (for simplicity, we use a grid identical to that employed to approximate density and viscosity). The derivatives with respect to coordinates in the heat equation are approximated by finite differences:

$$\frac{\partial T(t_n, x_1^i, x_2^j, x_3^k)}{\partial x_1} = \frac{T_{i+1,j,k}^n - T_{i-1,j,k}^n}{2h_1}, \quad h_1 = x_1^i - x_1^{i-1},$$

$$\frac{\partial^2 T(t_n, x_1^i, x_2^j, x_3^k)}{\partial x_1^2} = \frac{T_{i-1,j,k}^n - 2T_{i,j,k}^n + T_{i+1,j,k}^n}{h_1^2} = \Lambda_1(T^n)$$

(analogous formulas are used in the approximations along the x_2 and x_3 axes). On the domain boundary, the derivatives are approximated by introducing fictitious grid points [4]. The derivatives $\partial u_i / \partial x_j$ are determined by differentiating (2.1) and using (2.6).

Temperature is computed by an implicit alternating-direction method [4, 5]. Essentially, the values of $T^{n+1/3}$, $T^{n+2/3}$, and T^{n+1} are calculated on intermediate layers at each iteration step of the method as

$$T^{n+1/3} = T^n + \frac{\tau}{3} \left[\Lambda_1 \left(\frac{T^{n+1/3} + T^n}{2} \right) + \Lambda_2(T^n) + \Lambda_3(T^n) + U(T^n) \right],$$

$$T^{n+2/3} = T^{n+1/3} + \frac{\tau}{3} \left[\Lambda_1(T^{n+1/3}) + \Lambda_2 \left(\frac{T^{n+2/3} + T^{n+1/3}}{2} \right) + \Lambda_3(T^{n+1/3}) + U(T^{n+1/3}) \right],$$

$$T^{n+1} = T^{n+2/3} + \frac{\tau}{3} \left[\Lambda_1(T^{n+2/3}) + \Lambda_2(T^{n+2/3}) + \Lambda_3 \left(\frac{T^{n+2/3} + T^{n+1}}{2} \right) + U(T^{n+2/3}) \right],$$

where τ is the time step and U contains absolute terms, first derivatives of T , and the function T itself. In each iteration cycle in time, $n_2 n_3 + n_1 n_3 + n_1 n_2$ tridiagonal systems are solved, and the corresponding number of independent modules can be organized to perform parallel computations of these systems by a tridiagonal

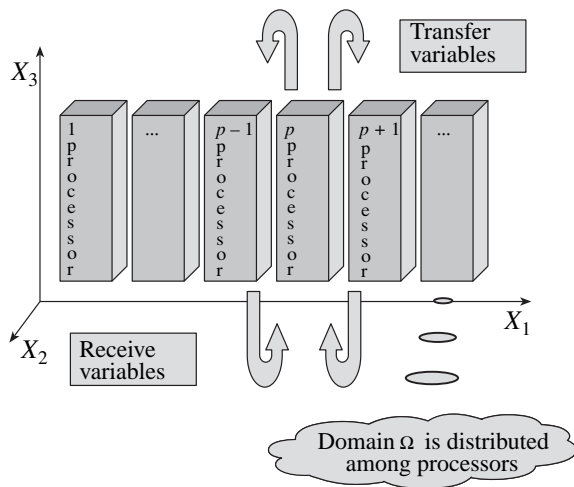


Fig. 2.

method. The representation of the vector velocity potential based on cubic splines employed here makes it possible to compute both convective transport and diffusion of temperature simultaneously by finite-difference methods.

2.5. The Scheme of Numerical Solution of the Overall Inverse Problem

The solution of the problem backwards in time consists of the following principal stages:

- (1) solution of a system of linear algebraic equations that determines the coefficients of the expansion of the vector velocity potential in terms of basis elements;
- (2) interpolation of the velocity field;
- (3) solution of the heat balance equation backwards in time;

- (4) solution of the advection equations for density and viscosity backwards in time.

Now, we describe the scheme of numerical solution of the overall inverse problem step by step. We define a uniform partition of the time axis at points $t_n = \vartheta - \tau n$ ($n \in \mathbb{Z}$), where τ is the time step. After that, we organize an iterative process in which n successively takes integer values from 0 to some natural number $m = \vartheta/\tau$. Each iteration cycle in time consists of the following three successive steps.

Step 1. Temperature $T = T(t_n, \cdot)$ and thermally unperturbed density $\rho_* = \rho_*(t_n, \cdot)$ and viscosity $\mu_* = \mu_*(t_n, \cdot)$ corresponding to $t = t_n$ are used in Eqs. (1.4) and (1.5) to find the thermally perturbed density $\rho = \rho(t_n, \cdot)$ and viscosity $\mu = \mu(t_n, \cdot)$ corresponding to the same $t = t_n$. Then, Eqs. (1.1) and (1.2) combined with appropriate boundary conditions are solved to find the potential $\psi = \psi(t_n, \cdot)$, and Eq. (2.1) is used to determine the velocity $\mathbf{u} = \mathbf{u}(t_n, \cdot)$.

Step 2. The velocity field $\mathbf{u} = \mathbf{u}(t_n, \cdot)$ and thermally perturbed density $\rho = \rho(t_n, \cdot)$ and viscosity $\mu = \mu(t_n, \cdot)$ are used in Eq. (1.3) combined with boundary conditions to find the temperature $T = T(t_{n+1}, \cdot)$ corresponding to $t = t_{n+1}$.

Step 3. The velocity field $\mathbf{u} = \mathbf{u}(t_n, \cdot)$ and thermally unperturbed density $\rho_* = \rho_*(t_n, \cdot)$ and viscosity $\mu_* = \mu_*(t_n, \cdot)$ are used in Eq. (1.6) to find the thermally unperturbed density $\rho_* = \rho_*(t_{n+1}, \cdot)$ and viscosity $\mu_* = \mu_*(t_{n+1}, \cdot)$ corresponding to $t = t_{n+1}$.

After the iterative process is completed, we will have temperature $T = T(t_n, \cdot)$, potential $\psi = \psi(t_n, \cdot)$, velocity field $\mathbf{u} = \mathbf{u}(t_n, \cdot)$, thermally unperturbed density $\rho_* = \rho_*(t_n, \cdot)$ and viscosity $\mu_* = \mu_*(t_n, \cdot)$, and thermally perturbed density $\rho = \rho(t_n, \cdot)$ and viscosity $\mu = \mu(t_n, \cdot)$ corresponding to $t = t_n$ ($n = 0, 1, \dots, m$). Having these results, we can use interpolation to reconstruct, when necessary, the entire process on the time interval $[0, \vartheta]$ in more detail. The time step is chosen automatically so that the maximal displacement of material points does not exceed a sufficiently small preset value. To solve the problem in a domain other than a parallelepiped, one can invoke the domain imbedding method [4].

3. NUMERICAL RESULTS FOR MODEL PROBLEMS

As model physical parameters of the medium, we take their values used in [14] (which are characteristic of the upper layers of the Earth).

Example 1. Consider the motion of an inhomogeneous viscous incompressible fluid in a gravity field within the parallelepiped $\bar{\Omega} = [0, 3] \times [0, 3] \times [0, 1]$. Set $T(t, x) = T_s$. At the initial time $t = 0$, an inclined fluid layer Ω_1 was located between two layers characterized by higher viscosity and density:

$$\Omega_1 = \{x \in \Omega : -0.05x_1 + 0.15 < x_3 < -0.05x_1 + 0.35 + 0.03 \sin(2\pi x_1) \sin(2\pi x_2)\}.$$

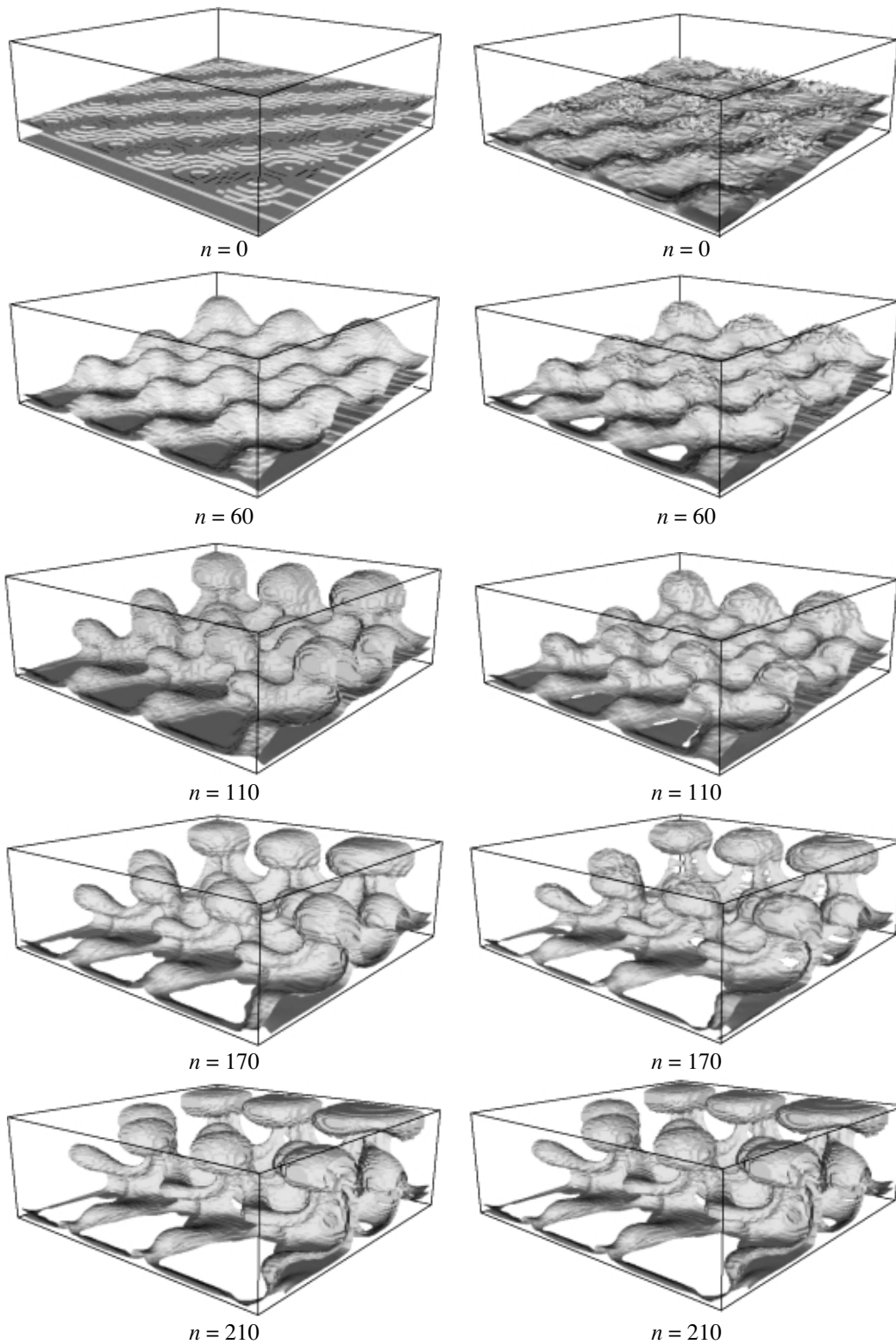


Fig. 3.

At the initial time, it was assumed that $\rho_0(x) = 0.85$ at $x \in \Omega_1$ and $\rho_0(x) = 1$ at $x \in \Omega/\Omega_1$, while $\mu_0(x) = 1$ at $x \in \Omega_1$ and $\mu_0(x) = 100$ at $x \in \Omega/\Omega_1$.

Disturbances of boundaries between the media were introduced as initial states of incipient diapirs, which would evolve in time as a result of the internal gravitational instability of the system. To be specific,

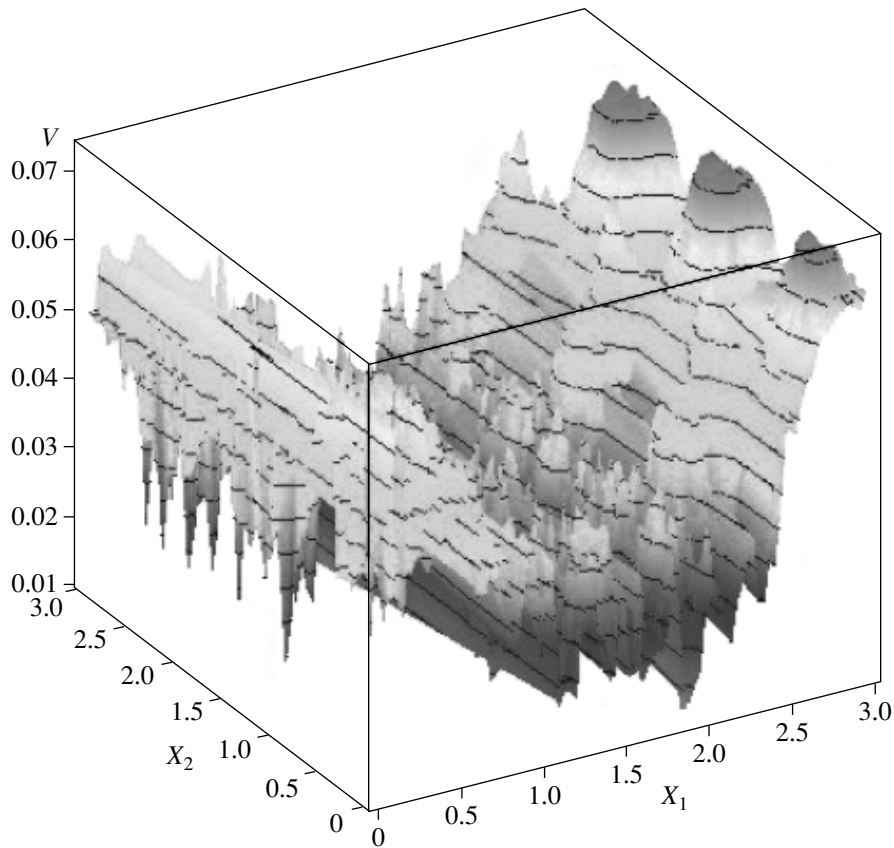


Fig. 4.

we restricted our analysis to the case of boundary conditions of perfect slip with impermeability for the Stokes problem.

To compute the problem, we used a $32 \times 32 \times 32$ grid in approximating the vector velocity potential and a $94 \times 94 \times 94$ grid in approximating density and viscosity. The corresponding system of linear algebraic equations was solved by using the parallel Gauss–Seidel algorithm. The run time required to compute an iteration cycle by means of ten processors was 2 min on an MVS-1000 distributed-memory parallel computer (including the computations of vector potential, velocity field, and updated density and viscosity).

The left-hand column in Fig. 3 shows the evolution of the fluid forward in time (evolution of diapirs). The depicted surface is the boundary between the light and heavy fluids. The right-hand column in the figure shows the time-reversed evolution of the diapirs (the reconstructed history of the diapirs). The final state of the model in the forward problem was used as the initial condition in the inverse problem.

Figure 4 shows the rms error (over the vertical axis)

$$v(x_1, x_2) = \left\{ \int_0^{l_3} [\rho_0(x_1, x_2, x_3) - \bar{\rho}_0(x_1, x_2, x_3)]^2 dx_3 \right\}^{1/2},$$

where $\bar{\rho}_0$ is the result obtained by solving the inverse problem.

Example 2. Consider fluid motion in the parallelepiped $\bar{\Omega} = [0, 3] \times [0, 3] \times [0, 1]$. At $t = 0$, we set $\rho_*(\cdot) \equiv 1$, $\mu_*(\cdot) \equiv 1$, and $T_0(x) = 1.1 - x_3/l_3$. We set $T_2(t, x) \equiv 0.1$ on the face $\Gamma(x_3 = l_3)$ and $T_1(t, x) \equiv 1.1$ on the face $\Gamma(x_3 = 0)$. For simplicity, we set $Q = 0$ and restricted our analysis to the case of boundary conditions of perfect slip with impermeability for the Stokes problem. The heat balance equation was supplemented by the boundary condition $\partial T/\partial \mathbf{n} = 0$ set on the lateral faces. To kick the fluid out of an unstable equilibrium,

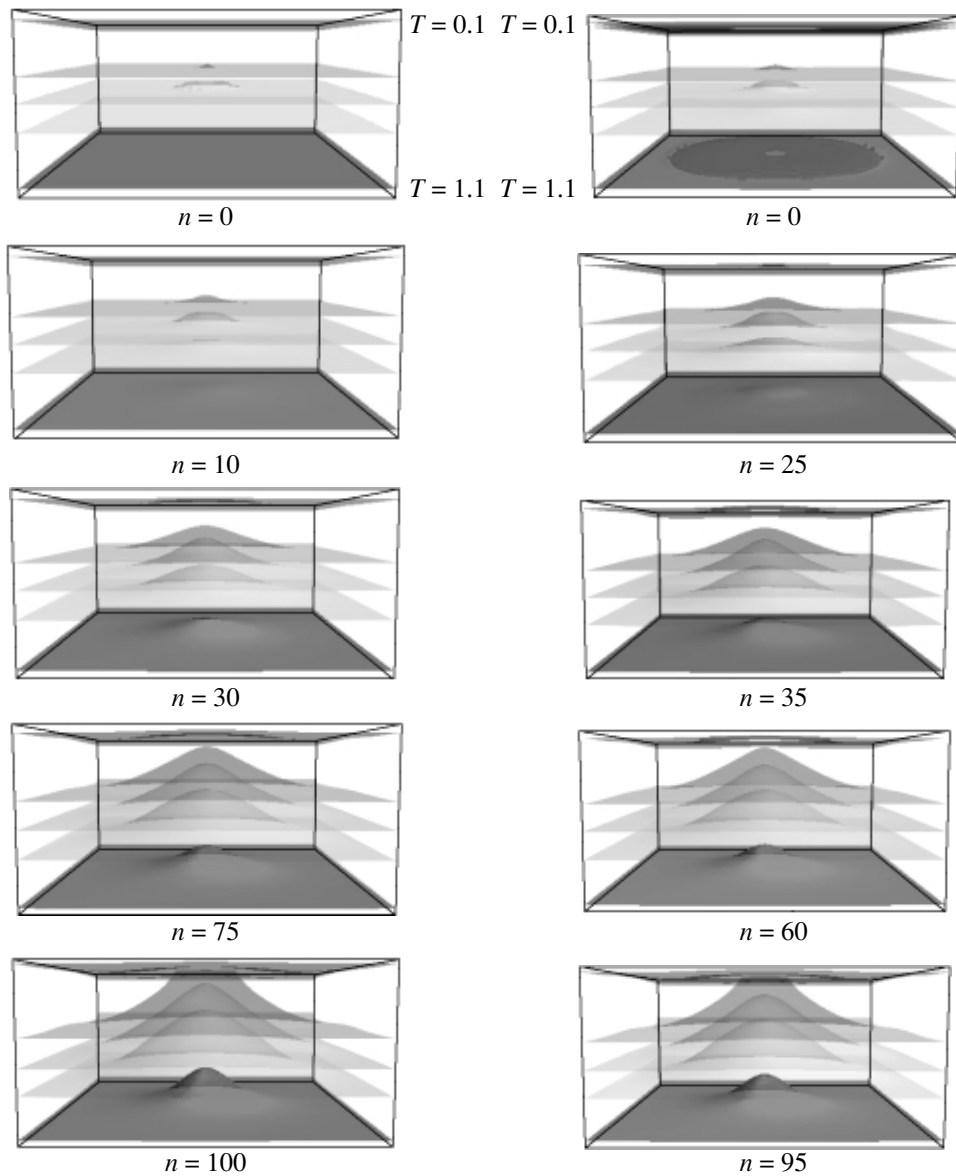


Fig. 5.

we introduced a small initial thermal disturbance at $x_0 = (3/2, 3/2, 1/3)$, which eventually developed into a diapir.

To compute the example, we used a $32 \times 32 \times 32$ grid in approximating the vector velocity potential and viscosity and a $94 \times 94 \times 94$ grid in approximating the density and temperature. The time step was set equal to 0.1.

The left-hand column in Fig. 5 illustrates the evolution of the fluid (evolution of the diapir) forward in time. The frames show the isotherms of $T = 0.1, 0.4, 0.7,$ and 1.0 at successive times. The right-hand column shows the isotherms corresponding to these temperature values computed backwards in time (as a reconstructed evolution of the diapir). The final state of the model in the forward problem was taken as the initial state in the inverse problem. Figure 6 shows the error

$$\delta T = |T_0(x_1, x_2, x_3) - \bar{T}_0(x_1, x_2, x_3)| = K,$$

where K is 0.01, 0.02, 0.04, or 0.08 and \bar{T}_0 is the result obtained by solving the inverse problem.

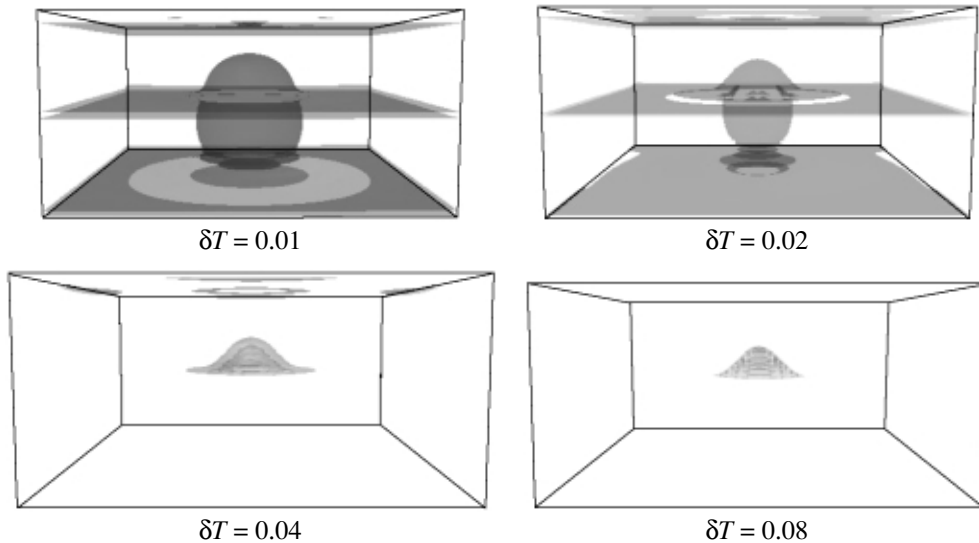


Fig. 6.

CONCLUSIONS

We proposed a numerical approach designed to solve the forward and inverse problems of three-dimensional slow motion of a viscous incompressible fluid with varying (temperature-dependent) density and viscosity induced by thermal and gravitational effects. Mathematically, we constructed a method of simultaneous approximate solution forward and backwards in time for the system consisting of the Stokes flow equation, incompressibility condition, heat equation, and advection equations for density and viscosity supplemented with appropriate boundary and initial conditions.

The basic results of this study are summarized as follows.

(1) A method for reconstructing an early state of the medium in question from its current state is proposed. The method is stable with respect to computational errors and inaccuracies.

(2) Typical examples of forward and inverse problems of gravitational instability and thermal convection were computed in the three-dimensional case.

ACKNOWLEDGMENTS

This work was supported by the Russian Foundation for Basic Research, project nos. 01-07-90210 and 02-01-00354, and by the International Science and Technology Center, project no. 1293-99.

REFERENCES

1. Chandrasekhar, S., *Hydrodynamic and Hydromagnetic Stability*, Oxford: Clarendon, 1961.
2. Landau, L.D. and Lifshits, E.M., *Gidrodinamika* (Fluid Dynamics), Moscow: Nauka, 1986.
3. Ladyzhenskaya, O.A., *Matematicheskie voprosy dinamiki vyazkoi neszhimaemoi zhidkosti* (Mathematical Topics in Viscous Incompressible Fluid Dynamics), Moscow: Nauka, 1970.
4. Marchuk, G.I., *Metody vychislitel'noi matematiki* (Methods of Computational Mathematics), Moscow: Nauka, 1989.
5. Tikhonov, A.N. and Samarskii, A.A., *Uravneniya matematicheskoi fiziki* (Equations of Mathematical Physics), Moscow: Nauka, 1972.
6. Ismail-zadeh, A.T., Kostyuchenko, S.L., and Naimark, B.M., The Timan-Pechora Basin (northeastern European Russia): Tectonic Subsidence Analysis and a Model of Formation Mechanism, *Tectonophysics*, 1997, vol. 283, pp. 205–218.
7. Naimark, B.M., Inverse Problem of Gravitational Stability, *Dokl. Akad. Nauk*, 1999, vol. 364, no. 4, pp. 1–3.
8. Ismail-zadeh, A.T., Naimark, B.M., and Talbot, C.J., Reconstruction of the History of a Fluid Motion: An Inverse Problem of Gravitational Stability, in *Vychislitel'naya seismologiya* (Computational Seismology), Moscow: Nauka, 2000, issue 31, pp. 52–61.

9. Ismail-zadeh, A.T., Talbot, C.J., and Volozh, Yu.A., Dynamic Restoration of Profiles Across Diapiric Salt Structures: Numerical Approach and Its Applications, *Tectonophysics*, 2001, vol. 337, pp. 23–38.
10. Korotkii, A.I., Tsepelev, I.A., Ismail-zadeh, A.T., *et al.*, Three-Dimensional Modeling of the Inverse Problem of Rayleigh–Taylor Instability, *Izv. Ural. Gos. Univ., Mat. Mekh.*, 2002, vol. 22, no. 4, pp. 85–95.
11. Naimark, B.M., The Existence and Uniqueness of a Solution to the Rayleigh–Taylor Instability Problem, in *Vychislitel'naya seismologiya* (Computational Seismology), Moscow: Nauka, 1986, issue 18, pp. 35–45.
12. Naimark, B.M., The Existence and Uniqueness of a Local Solution to the Rayleigh–Taylor Instability Problem, in *Vychislitel'naya seismologiya* (Computational Seismology), Moscow: Nauka, 1988, issue 21, pp. 94–114.
13. Korotkii, A.I., Tsepelev, I.A., Ismail-zadeh, A.T., *et al.*, Parallel Algorithms for Simulation of Thermal Convection in a Viscous Fluid, *Izv. Ural. Gos. Univ., Mat. Mekh.*, 2000, vol. 17, no. 3, pp. 65–79.
14. Ismail-zadeh, A.T., Korotkii A.I., Naimark B.M., *et al.*, Numerical Simulation of Three-Dimensional Viscous Flows with Gravitational and Thermal Effects, *Zh. Vychisl. Mat. Mat. Fiz.*, 2001, vol. 41, no. 9, pp. 1399–1415.
15. Ismail-zadeh, A.T., Korotkii, A.I., Naimark, B.M., *et al.*, Implementation of a Three-Dimensional Hydrodynamic Model for Evolution of Sedimentary Basins, *Zh. Vychisl. Mat. Mat. Fiz.*, 1998, vol. 38, no. 7, pp. 1190–1203.
16. Naimark, B.M., Ismail-zadeh, A.T., Korotkii, A.I., *et al.*, Numerical Implementation of a Three-Dimensional Hydrodynamic Model for Evolution of Sedimentary Basins, *Tr. Inst. Mat. Mekh. Ural. Otd. Ross. Akad. Nauk*, 1998, vol. 5, pp. 142–172.
17. Korotkii, A.I., Tsepelev, I.A., Ismail-zadeh, A.T., *et al.*, Parallel Algorithms for Simulation of Inhomogeneous Viscous Flows, *Izv. Ural. Gos. Univ., Mat. Mekh.*, 1999, vol. 2, no. 14, pp. 65–76.
18. Naimark, B.M., Ismail-zadeh, A.T., Korotkii, A.I., *et al.*, Simulation of Three-Dimensional Viscous Flows in Upper Mantle Layers, in *Vychislitel'naya seismologiya* (Computational Seismology), Moscow: GEOS, 1998, issue 30, pp. 3–15.
19. Vasil'ev, V.V., *Metody resheniya ekstremal'nykh zadach* (Solution Methods for Extremum Value Problems), Moscow: Nauka, 1981.